ANALYSIS OF STRESS APPLIED TO FUEL CLADDING BY HORIZONTAL VIBRATION UNDER POST-LOCA CONDITION

K. KITANO and M. OZAWA
Regulatory Standard and Research Department, Secretariat of Nuclear Regulation Authority (S/NRA/R), Roppongi 1-9-9, Minato-ku, Tokyo, 106-8450 Japan

ABSTRACT

After the termination of a LOCA, the reactor should continue to be cooled for a long term. The strength of the fuel cladding decreases due to high-temperature oxidation, ballooning, burst and quenching during the LOCA event, so whether the post-LOCA integrity of the fuel rods is sufficient to withstand earthquakes during the cooling is a concern in terms of preservation of a reactor core coolable geometry. In order to investigate the post-LOCA aseismic performance of fuel rods, FEM analysis was performed to estimate stress applied to fuel cladding with a burst opening when a fuel rod was vibrated horizontally displacing the both ends. The analysis showed that stress was localised at the side edge of the burst opening. However, the localised stress was lower than the strength assessed from bending tests of cladding samples which experienced burst and oxidation to <15%ECR at 1200°C in advance. Therefore, it is expected that fuel rods likely survive earthquakes during the post-LOCA cooling if the cladding is oxidised below the limit defined in the current Japanese LOCA criteria.

1. Introduction

In a loss-of-coolant accident (LOCA), fuel rods are exposed to high temperature oxidation and the following thermal shock by emergency core cooling water. The fuel cladding is ballooned and burst depending on the temperature and rod internal pressure prior to the high temperature oxidation phase. Many studies have been conducted on the ductility and strength of cladding which has been ballooned, burst and oxidised under LOCA conditions in order to verify preservation of a coolable geometry of the reactor core in a LOCA [1].

After the termination of a LOCA, the reactor should continue to be cooled for a long term. The strength of the fuel cladding after the LOCA event decreases due to high temperature oxidation, ballooning and burst. Mechanical load applied to fuel assemblies and fuel rods is expected during the long-term cooling. Considering the accident at the TEPCO Fukushima Dai-ichi NPP [2], where earthquakes occurred following the main one, the earthquake may be one of the greatest causes of the mechanical load to fuel rods after the LOCA event. Then it is a concern whether the post-LOCA integrity of the fuel rods is sufficient to withstand earthquakes during the long-term cooling in terms of preservation of a core coolable geometry. In other words, it is necessary to consider the coolability during the post-LOCA phase as well as during the LOCA transition.

The objective of this study is to investigate the aseismic performance of a fuel rod during the post-LOCA phase. Finite element method (FEM) analysis was performed to analyse the stress applied to the fuel cladding with a burst opening under vibration conditions. The analysed stress was then compared with the cladding strength assessed from bending tests for ballooned, burst, and oxidised cladding samples [3] in order to evaluate the post-LOCA aseismic performance of the fuel rod.

2. Modelling for finite element method analysis

2.1 Geometry of burst opening

FEM analyses were performed using a general FEM analysis code, ABAQUS [4]. First, the geometry of the ballooned cladding was formed by the internal pressurisation of an intact 17x17 type PWR cladding tube with an axial temperature gradient of 0.3°C/mm in a FEM analysis. The 17x17 type PWR cladding tube had an outer diameter of 9.5 mm and an inner diameter of 8.36 mm. The FEM model of the cladding consisted of solid elements. Next, a

cladding tube burst was simulated by the application of an axial line of solid elements that fractured at a threshold plastic strain of 20%. Figure 1 shows the created burst cladding model together with a picture of the typical appearance of a burst cladding tube after a LOCA test. The shape of the ballooned and burst cladding is well reproduced by the FEM analysis. The burst cladding model in Fig.1 (b) that had a strain of approximately 40 % at a maximum was used in the following analyses of this study.

(a) Cladding tube after LOCA test [5]

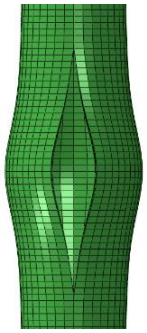

(b) FEM model of burst cladding tube

Fig. 1 Appearances of a burst cladding sample and FEM model

2.2 Adjustment of mechanical property

Initial values of the mechanical properties used in the FEM code are nominal values for non-oxidised Zircaloy. To calculate mechanical responses of the burst and oxidised fuel cladding during the post-LOCA conditions, appropriate mechanical properties should be used in the FEM calculation. For that, the mechanical properties of the cladding were adjusted so that the results of the FEM analysis of the bending test fit with the test results. The analysis was done for the bending test that was performed at 135°C by ANL for an intact cladding sample of ZIRLO (without ballooning and burst) oxidised at 1200°C and 17% Cathcart-Pawel (CP) - equivalent cladding reacted (ECR) [6]. Figure 2 shows the configuration of the FEM analysis of the bending test. Figure 3 shows load-displacement curves obtained from the test and the FEM analyses with different Young's modules. Based on the comparison in Fig.3, a Young's modulus of the oxidised cladding at 135°C was set at 89 GPa. In this analysis, the Poisson's ratio was assumed to be 0.3.

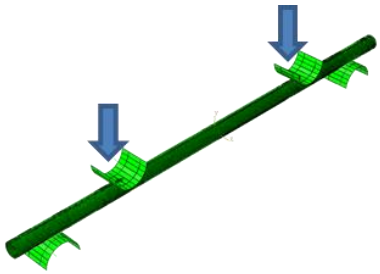

(a) Model of bending test

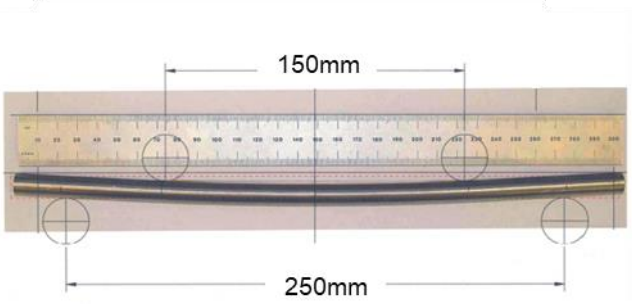

(b) Dimensions of test configuration[6]

Fig. 2 Configuration of bending test for analysis

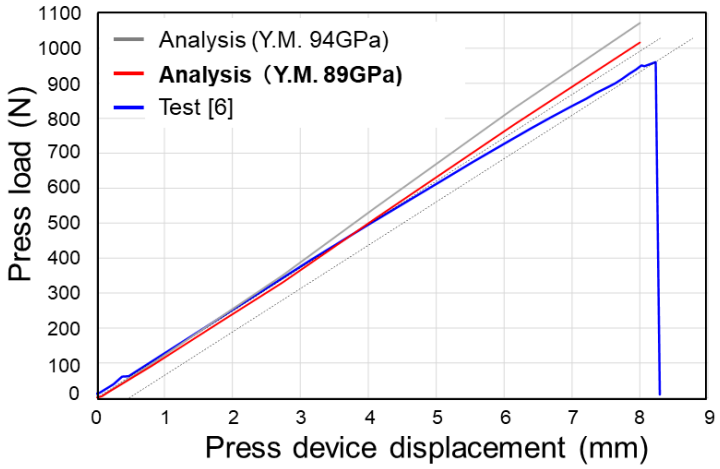

Fig. 3 Analysis results and test result for intact cladding sample

2.3 Validation of burst geometry and mechanical property

The FEM model geometry with a bust opening and the material properties for an oxidized cladding tube were validated through a comparison of analysis results with test results on burst and oxidised cladding samples [5]. The configuration of the bending tests was the same as in Fig. 2. The burst opening was placed at the centreline and facing down. Figure 4 shows the results of the FEM analysis and two tests for burst cladding samples oxidised to 13 and 17% CP-ECR. The test results shown in Fig. 4 are shifted from the original results [5] to eliminate the influence of looseness of the test device in displacement measurements in the initial stage of the tests, so that they close to a line through the origin. The test results show that the two samples failed at about 200 and 300 MPa, respectively. The FEM analysis cannot simulate the failure but it simulates well the deformation of the burst and oxidised cladding samples that corresponds to the relation between load and displacement. Consequently, Fig. 4 demonstrates that the FEM model was adequate to analyse mechanical response of the burst and oxidised cladding.

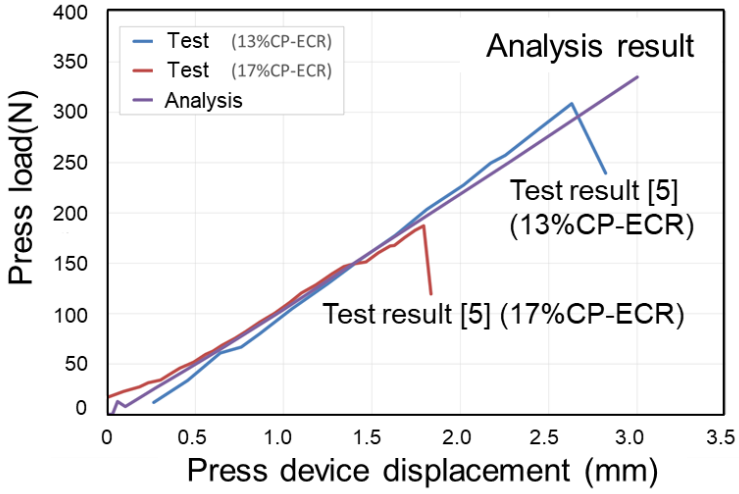

Fig. 4 Analysis result and test results for burst and oxidised sample

2.4 Stress distribution in burst cladding sample in bending test

Figure 5 shows stress distribution on the axial cross section of the burst cladding sample with a burst opening facing down. Tensile stress is localised at the opening. This result agrees with the test results that the burst cladding sample fails at the opening position in the bending tests [5]. Figure 6 shows the analysed load- displacement curves in the bending tests for burst cladding samples with an opening facing both up and down, and also for an intact cladding sample. The burst opening degrades the mechanical stiffness. In addition, the mechanical stiffness depends on the azimuthal directions of the burst opening. The case with the opening

facing up indicates a lower stiffness than that facing down. When the opening is facing down, the opening gradually closes as bending progresses. When the opening is facing up, on the other hand, the opening widens as bending progresses. This difference results in a mechanical stiffness difference.

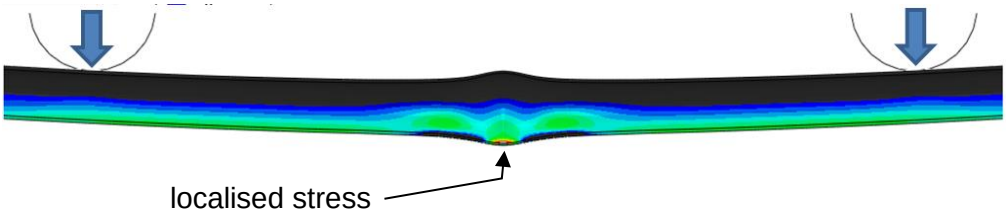

Fig. 5 Stress distribution on the axial cross section of a burst cladding sample in a bending test

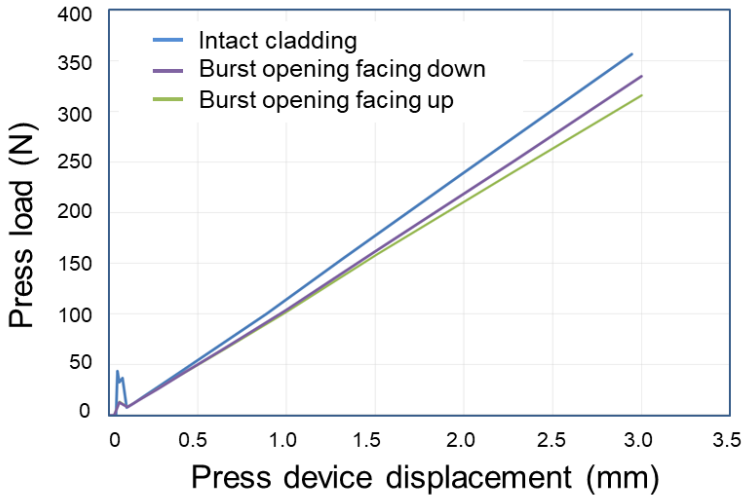

Fig. 6 Mechanical stiffness depending on the azimuthal direction of the burst opening

2.5 Fuel rod model in vibration analysis

A full-length 17x17-type PWR fuel rod with nominal dimensions at fabrication was modelled with all the components including the cladding, fuel pellets, end plugs and plenum spring. The burst opening shown in Fig.1 (b) was placed at the middle of the fuel rod. First, the full model considered friction between pellet and pellet, and also friction and impact between pellet and cladding. However, the time required for analysis was too long. Then a “combined” model was developed to solve the problem. The pellet-pellet gaps and pellet-cladding gaps were filled with a soft elastic body, therefore, the cladding and pellets were unified in the combined model. Figure 7 shows displacement histories calculated with the full model and combined model, where the displacement is defined as the difference in relative position in the horizontal direction between the middle of the rod and both ends, in the vibrated fuel. The two displacement histories are similar. Since it was confirmed by the analysis on the vibration behaviours that the two models provided the similar results, the combined model was used in the following vibration analysis.

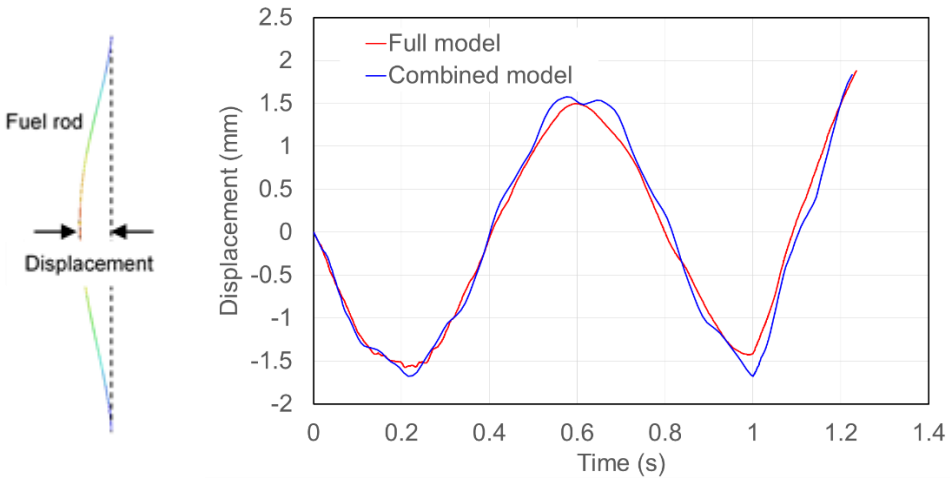

Fig. 7 Displacement histories in the vibrated fuel calculated with the full model and combined model

2.6 Vibration condition

Fuel assemblies in a core are shaken by the upper and lower core plates in an earthquake event. In this study, both ends of the fuel rod were simultaneously displaced in the X-direction, i.e. horizontal direction with a constant acceleration to simulate vibration under the characteristic frequency of the first mode that gives the severest deformation in an earthquake event. The top end was fixed to the Y-direction and Z-direction, where the Z-direction was defined as the axial direction along the fuel rod. The bottom end was fixed only to the Y-direction and allowed to displace to the Z-direction. Temperature was assumed to be 135°C, which is the typical coolant saturation temperature following core quenching.

3. Results

3.1 Vibration characteristics

Figure 8 shows calculated displacement, which is defined as the difference in relative position in the X-direction between the middle of the rod and both ends, in the vibrated fuel rod. Since the fuel rod was vibrated with the first mode characteristic frequency with a constant acceleration, the peak displacement increases with time. Analyses were performed for the intact rod and ballooned cladding rod as well as the burst cladding rods with different azimuthal angles between the opening and the vibration direction, however, the displacement changes with time were identical in all the analysed cases, as in Fig. 8. This indicates that there is no effect of ballooning and burst on the overall vibration characteristics of a fuel rod, despite the difference in mechanical stiffness as shown in Fig.6. That is likely to be because the range of the ballooning and burst as shown in Fig.1 is too small to affect the vibration characteristics of the fuel rod of an approximately 4 m long.

3.2 Stress applied to cladding

Figure 9 shows results of vibration tests with full-scale PWR fuel assemblies [7]. It indicates that the maximum displacement of the fuel assembles is limited to 40 – 50 mm even at higher input accelerations due to contact with the adjacent core structures and fuel assemblies. Therefore, stress applied to the fuel cladding at the displacement peak of 58 mm in Fig. 8 was analysed with consideration given to conservativeness.

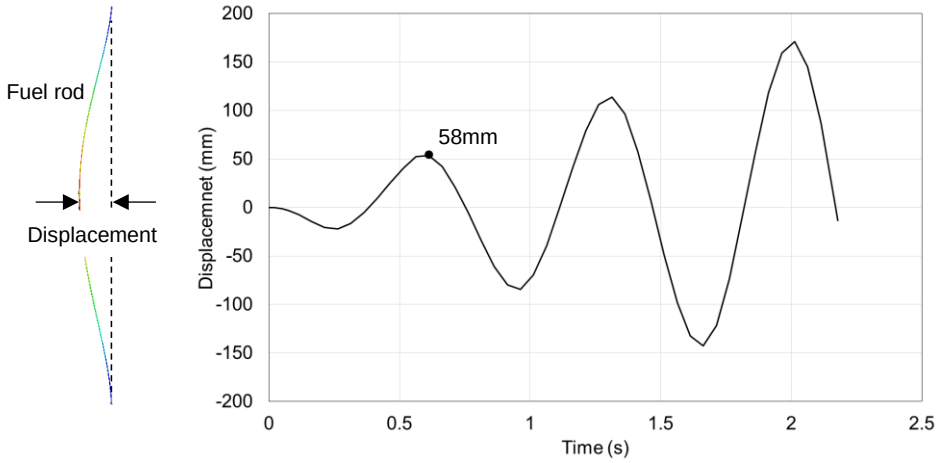

Fig. 8 Displacement, which is defined as relative position in the horizontal direction between the middle of the rod and the both ends, versus time

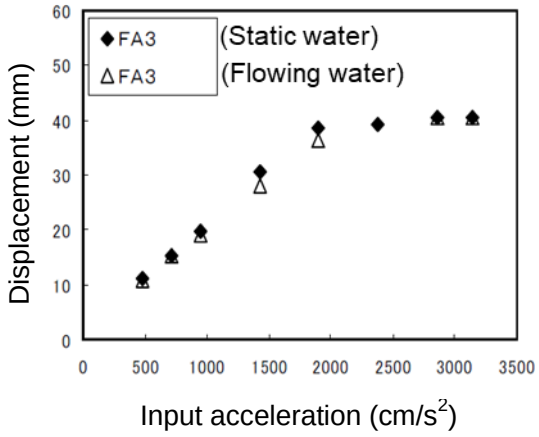

Fig. 9 Results of the vibration test for multi-assemblies of PWR fuel [7]

Table 1 lists the maximum principal stresses in the intact rod, ballooned cladding rod and burst cladding rods with different azimuthal angles between the burst opening and vibration direction. The largest stress, 68 MPa is observed when the directions of vibration and opening are identical. On the intact rod and ballooned cladding rod, the maximum stress of 27.5 MPa was generated at the position corresponding to a pellet-pellet interface.

Table 1 Maximum stress analysed in cladding at a displacement of 58mm

Cladding condition	Angle between opening and vibration (Degree)	Maximum principal stress (MPa)	Location of maximum stress
Intact	-	27.5	Intact part
Ballooned	-	27.5	Intact part
Burst	0	68.0	Middle of opening
Burst	90	28.3	Edge of opening
Burst	45	50.1	Edge of opening

Figure 10 shows distributions of axial (Z-direction) component of stress in the burst cladding when the directions of vibration and opening are identical and 45º different. Figure 10 (a) shows that tensile stress is localised at the middle of the burst opening while compression stress is observed at both ends of the opening. The maximum axial stress component is 68 MPa which is identical to the maximum principal stress in 0º case in Table 1. This indicates that uniaxial stress in the axial direction (Z-direction) is applied there. The stress distribution is similar to that obtained in the analysis of the bending test (Fig. 5).

Figure 10 (b) shows that tensile stress is localised at the edge and side of the opening. The maximum axial component is 43 MPa which is slightly different from the maximum principal stress of 50.1 MPa in Table 1. This means that there is a contribution of other stress components.

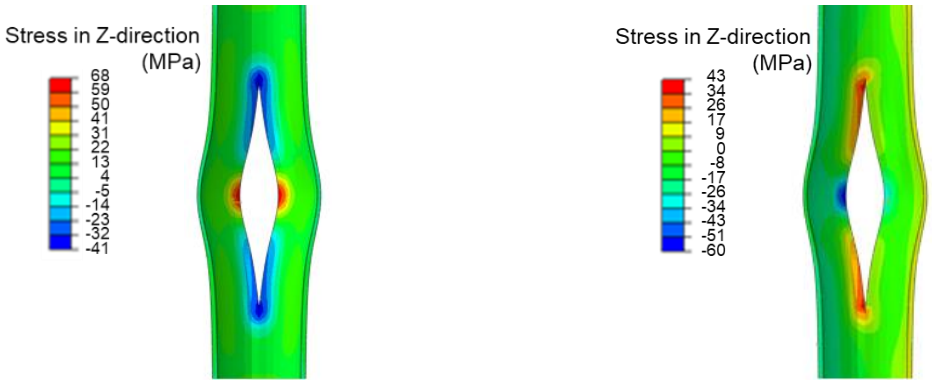

(a) 0 º case (b) 45º case

Fig. 10 Stress distribution in burst cladding

3.3 Comparison with test results

Figure 11 shows the results of bending tests performed by JAEA [3]. Burst cladding samples were oxidised to different ECRs calculated with Baker-Just correlation at the four temperatures and then quenched before the bending tests. The bending tests were conducted at 135ºC. Data points plotted in Fig.11 exhibit the maximum bending moment measured in each bending test. The burst cladding samples that had been treated below the 15%ECR (the oxidation limit in the Japanese LOCA criteria) fractured at greater than about 8 Nm.

The bending moment can be converted to tensile stress using the following equation.

$$\sigma = \frac{Mr}{I} \qquad (1)$$

σ : Tensile stress (N/m^2)
M : Bending moment (Nm)
r : Cladding radius (m)
I : Area moment of inertia (m^4)

The bending moment of 8 Nm corresponds to a tensile stress of about 200 MPa (=2x10^{8}N/m^2) according to the equation (1). Consequently, the results of the JAEA's bending tests suggest that the burst cladding oxidised to <15%ECR withstands a stress of 200 MPa. As described in 3.2, the highest stress applied to the burst cladding is 68 MPa at a conservative displacement of 58 mm under vibration in the analyses. Accordingly, the burst cladding likely survives earthquakes during the post-LOCA long-term cooling when the cladding oxidation is below the current Japanese LOCA criterion.

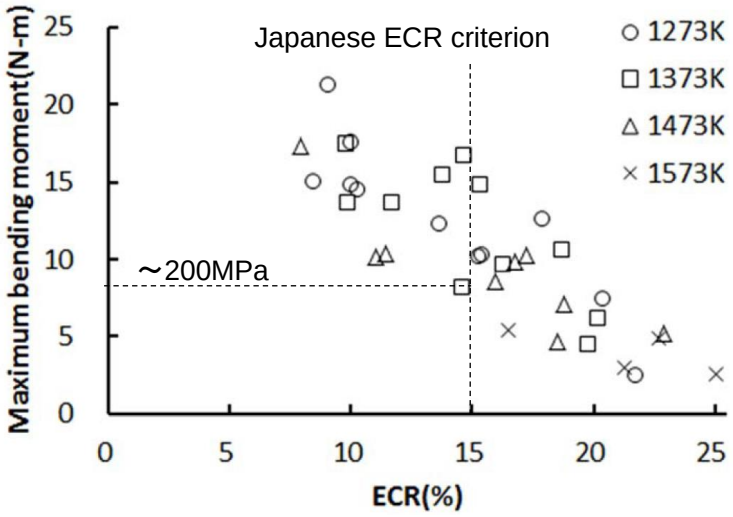

Fig. 11 Maximum bending moment from test for burst cladding sample after LOCA-simulated oxidation[3]

4. Conclusion

FEM analysis was performed to estimate stress applied to cladding with a burst opening under vibration. The analysis showed that stress was localised at the side edge of the burst opening. However, the localised stress was lower than the strength assessed from the bending test of the cladding sample with a burst opening after oxidation at 1200°C to <15%ECR. The conclusion in this study is that fuel rods would likely survive earthquakes during the post-LOCA cooling when the cladding oxidation is below the current Japanese LOCA criterion (15%ECR). However, stress applied to the fuel cladding was analysed under simplified vibration conditions to roughly estimate the integrity of the fuel rod during the post-LOCA cooling in this study. In reality, cyclic load is applied to the fuel cladding and the vibration mode would be complicated during earthquakes. Therefore, additional studies are necessary, for example, to evaluate the fatigue strength of the cladding which experienced the LOCA conditions in order to confirm that the current Japanese LOCA criterion is sufficient to prevent post-LOCA cladding from fatigue failure during earthquakes so that the core coolability after the LOCA event is preserved.

Reference

[1] OECD NEA Working Group on Fuel Safety, “Nuclear fuel behavior in loss-of-coolant accident (LOCA) conditions, State-of-the-art report”, NEA/CSNI/R(2009)15, OECD NEA, No. 6846, ISBN 978-92-64-99091-3.

[2] IAEA, “The Fukushima Daiichi Accident, Report by the Director General”, GC(59)/14, Aug. 2015, ISBN 978–92–0–107015–9.

[3] M. Yamato, et al., “Evaluation of fracture resistance of ruptured, oxidized, and quenched Zircaloy cladding by fourpoint-bend tests” Journal of Nuclear Science and Technology Vol. 51 , Iss. 9, (2014)

[4] Dassault Systemes, ABAQUS version 6.14, https://www.3ds.com/products-services /simulia/products/abaqus/

[5] U.S. NRC, “Mechanical behavior of ballooned and ruptured cladding”, NUREG-2119, Feb. 2012

[6] U.S. NRC, “Assessment of current test methods for post-LOCA cladding behavior”, NUREG/CR-7139, Aug. 2012

[7] JNES, “Report for testing and investigation for evaluation technology of aseismic performance of nuclear facilities, Component strength part-2 (insertability of PWR control rod)”, 06 基構報-0001, Aug. 2006 (in Japanese)